Supplementary Information

Active Lattice Oxygen in Co-doped $SrTiO_3$ on CO Oxidation Based on Mars–van Krevelen Mechanism

Ryosuke Sugimoto,[a] Yuta Odani,[a] Saki Imada,[b] Saburo Hosokawa*,[a]

[a] Faculty of Materials Science and Engineering, Kyoto Institute of Technology, Matsugasaki, Sakyo-ku, Kyoto 606-8585, Japan

[b] Faculty of Electrical Engineering and Electronics, Kyoto Institute of Technology, Matsugasaki, Sakyo-ku, Kyoto 606-8585, Japan

***Corresponding Author**

E-mail address: hosokawa@kit.ac.jp (S.H.)

Table S1. BET surface areas of $SrTi_{1-x}Co_xO_3$ and Pt/Al_2O_3.

Sample	BET surface area / $m^2\ g^{-1}$
$SrTiO_3$	5
$SrTi_{0.98}Co_{0.02}O_3$	11
$SrTi_{0.9}Co_{0.1}O_3$	4
$SrTi_{0.8}Co_{0.2}O_3$	2
$SrTi_{0.7}Co_{0.3}O_3$	2
$SrTi_{0.6}Co_{0.4}O_3$	2
$SrTi_{0.4}Co_{0.6}O_3$	1
$SrTi_{0.2}Co_{0.8}O_3$	1
Pt/Al_2O_3	105

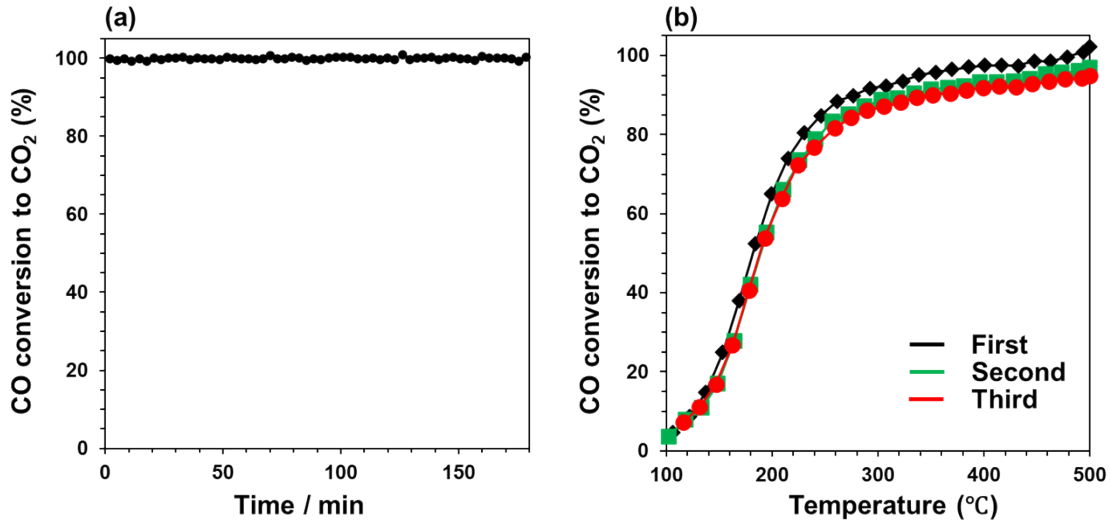

Figure S1. Results of the (a) durability test at 300℃ and (b) cycling stability tests of CO oxidation over $SrTi_{0.8}Co_{0.2}O_3$.

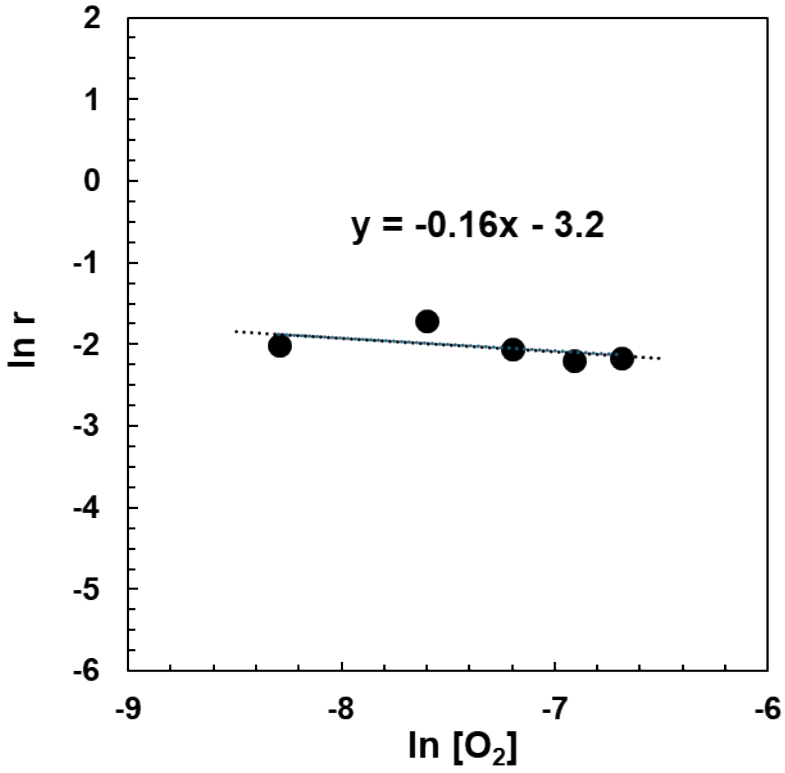

Figure S2. Reaction order on the $SrTi_{0.2}Co_{0.8}O_3$ catalyst with respect to oxygen partial pressure.

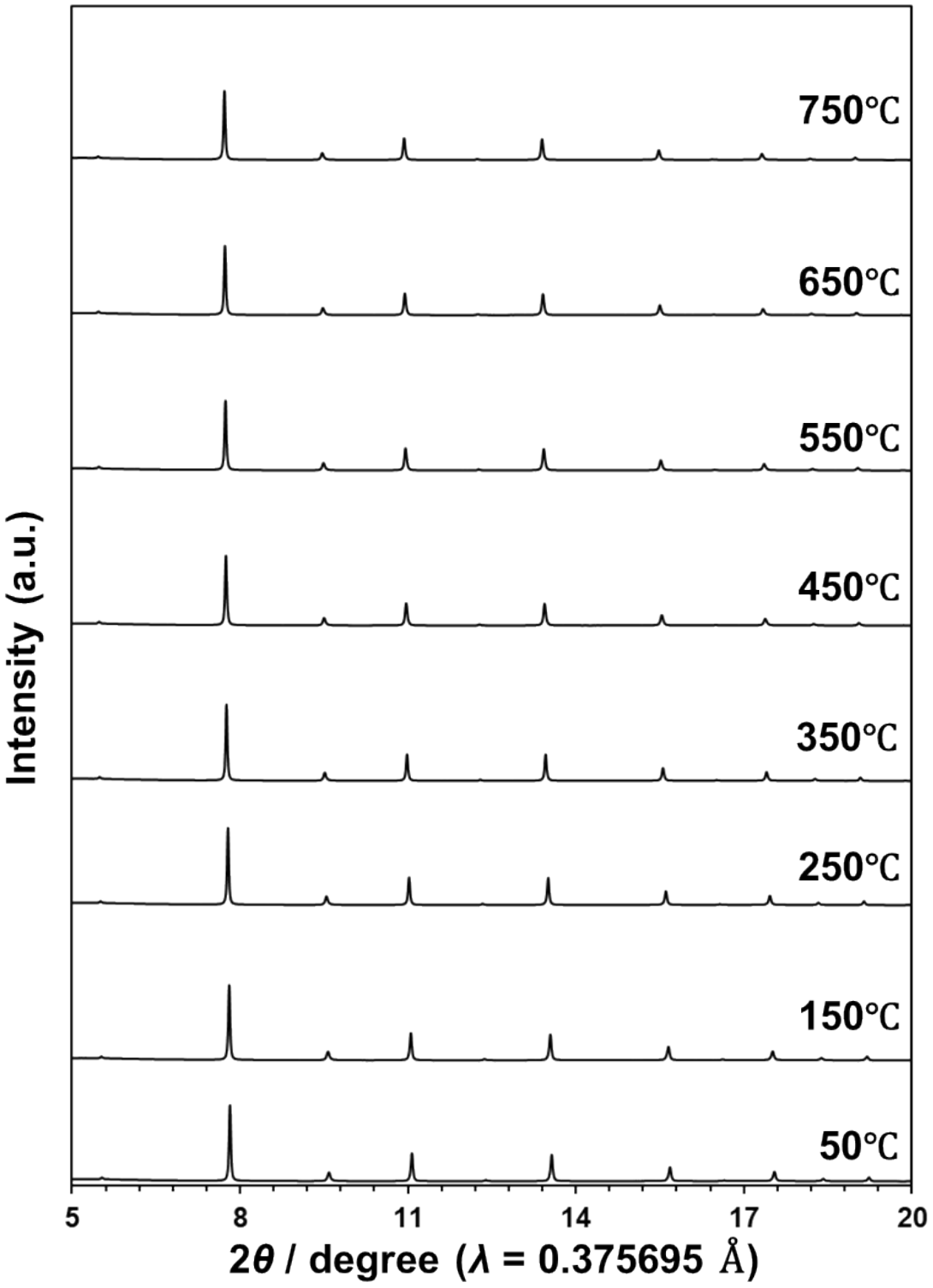

Figure S3. *In situ* two-dimensional XRD patterns of $SrTi_{0.8}Co_{0.2}O_3$ in an H_2 atmosphere.

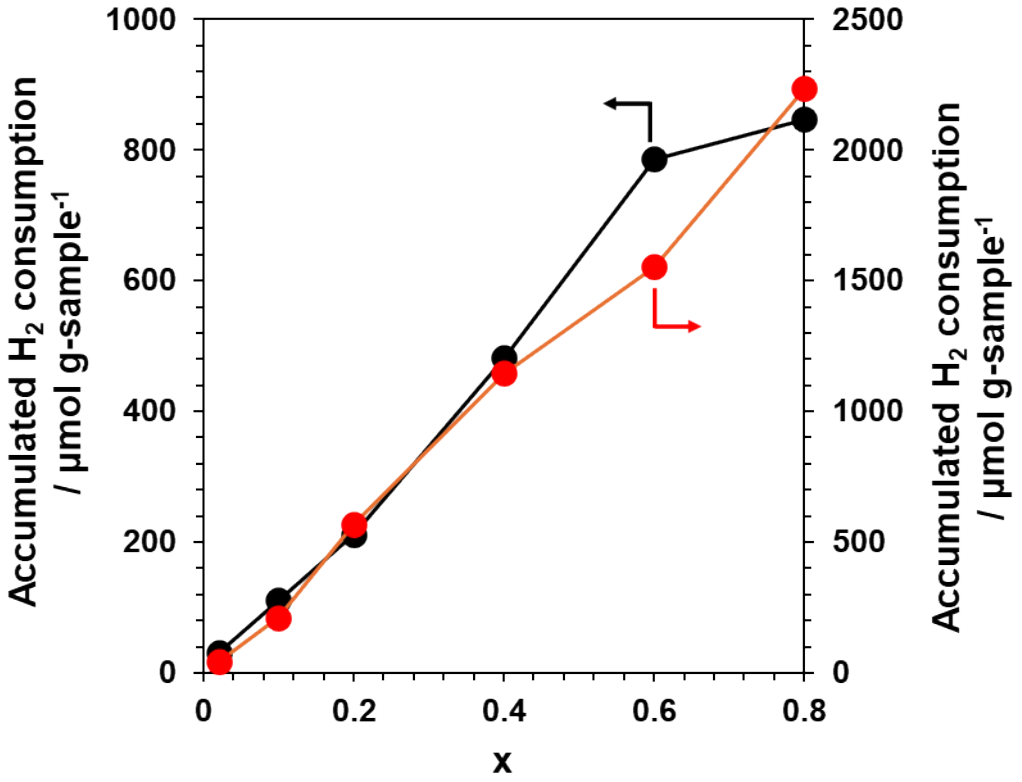

Figure S4. Accumulated H_2 consumption for $SrTi_{1-x}Co_xO_3$ (x = 0.02, 0.1, 0.2, 0.3, 0.4, 0.5, 0.6 and 0.8) at reduction peak (i) (black) and reduction peak (ii) (red).

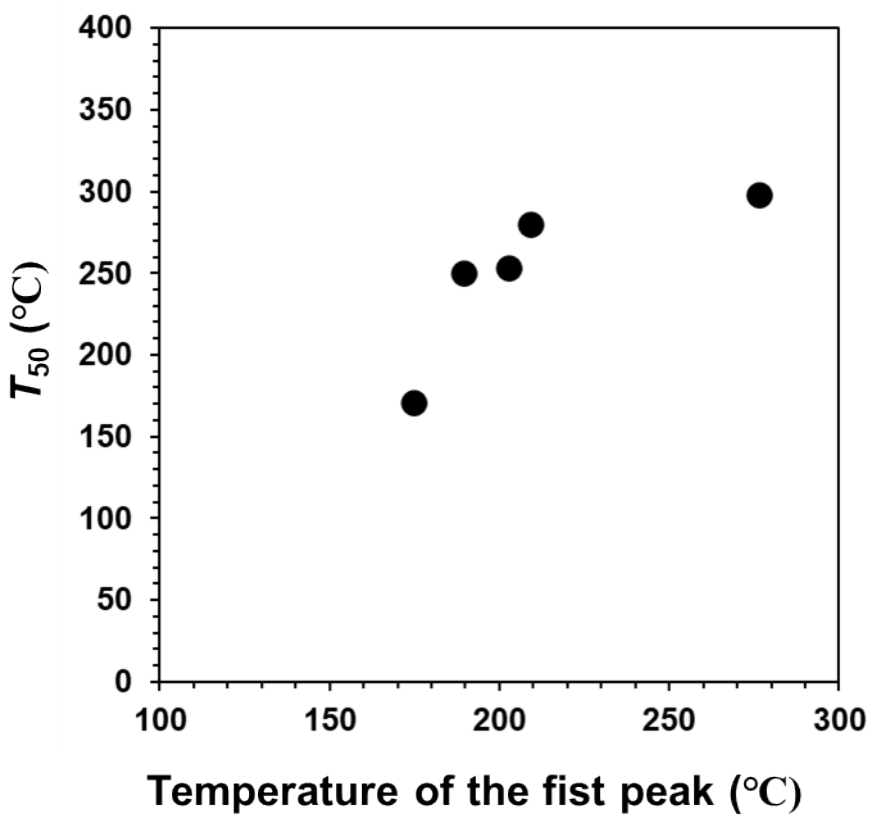

Figure S5. Relationship between the temperature of the first peak in H_2-TPR and T_{50}.

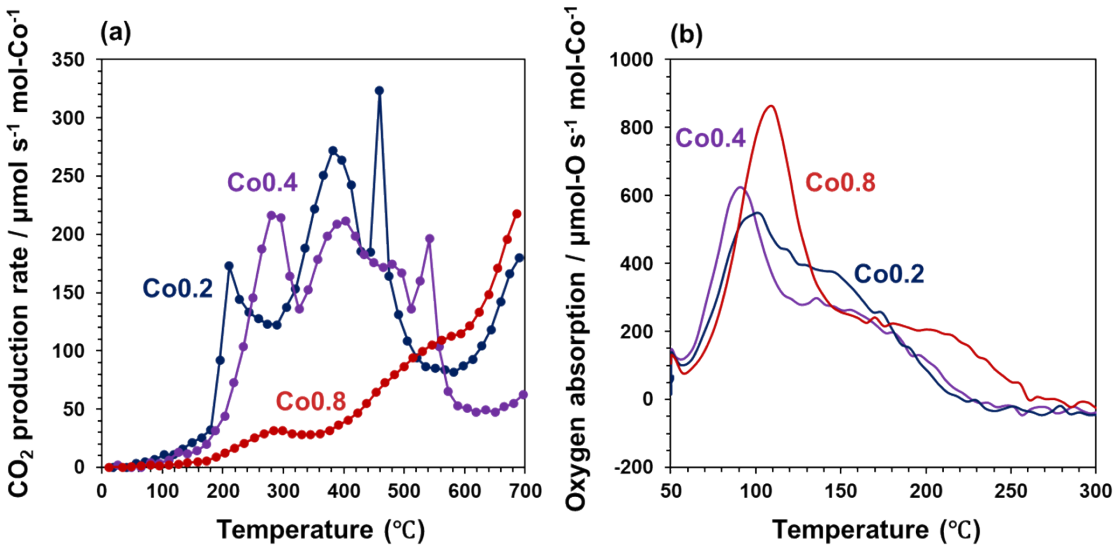

Figure S6. (a) CO-TPR and (b) O_2-TPO over $SrTi_{1-x}Co_xO_3$ (x =0.2, 0.4, and 0.8).

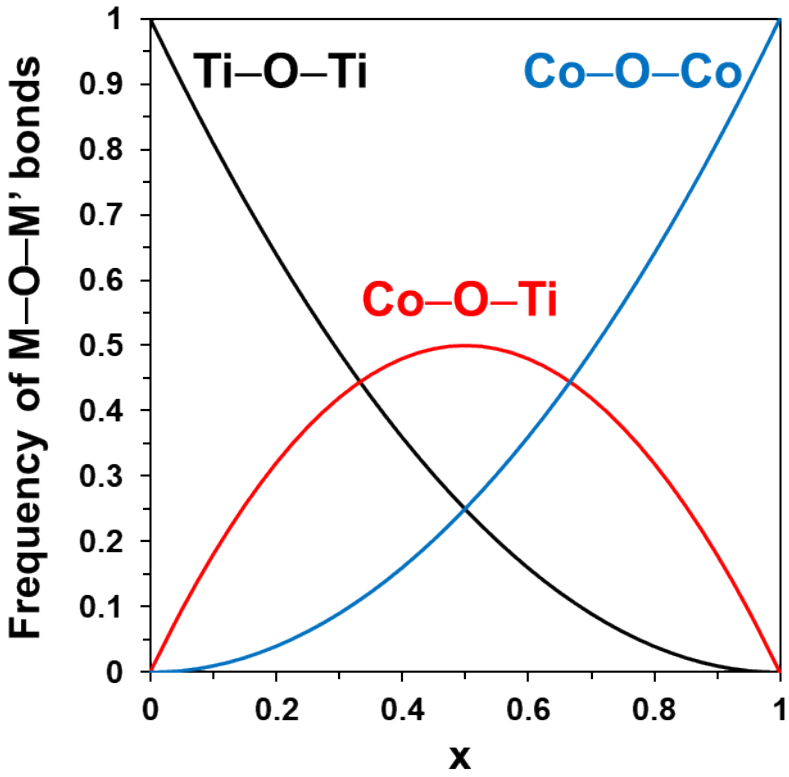

Figure S7. Estimated relative frequencies of M–O–M' bonds based on statistical analysis. Relative frequencies of the Co–O–Co, Ti–O–Ti, and Co–O–Ti bonds are calculated assuming that Co and Ti occupy the B site with probabilities of x and 1–x, respectively, resulting in frequencies given by x^2, $(1–x)^2$, and $2x(1–x)$, respectively.

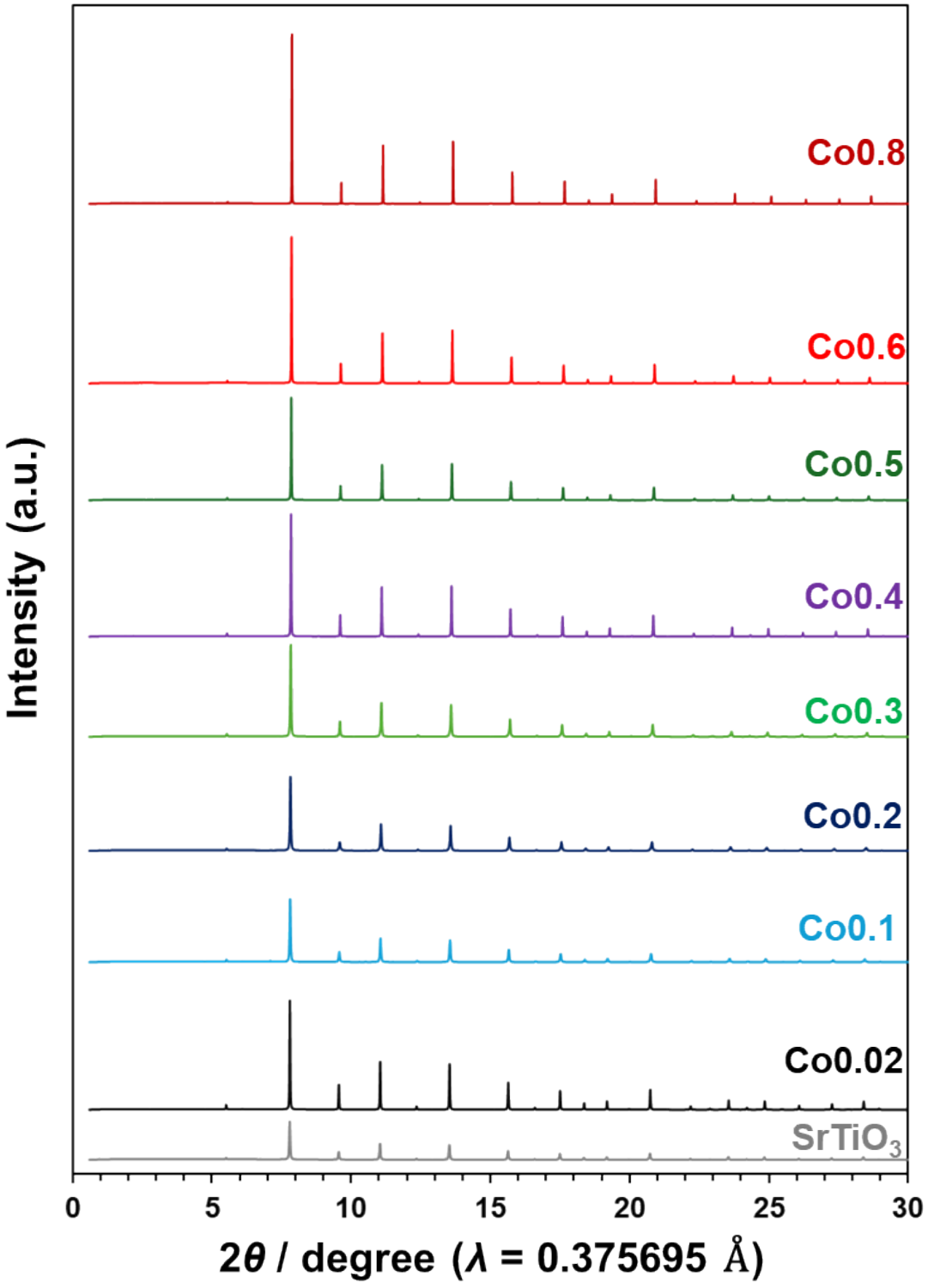

Figure S8. Synchrotron XRD patterns at room temperature of $SrTi_{1-x}Co_xO_3$ (x = 0, 0.02, 0.1, 0.2, 0.3, 0.4, 0.5, 0.6 and 0.8).

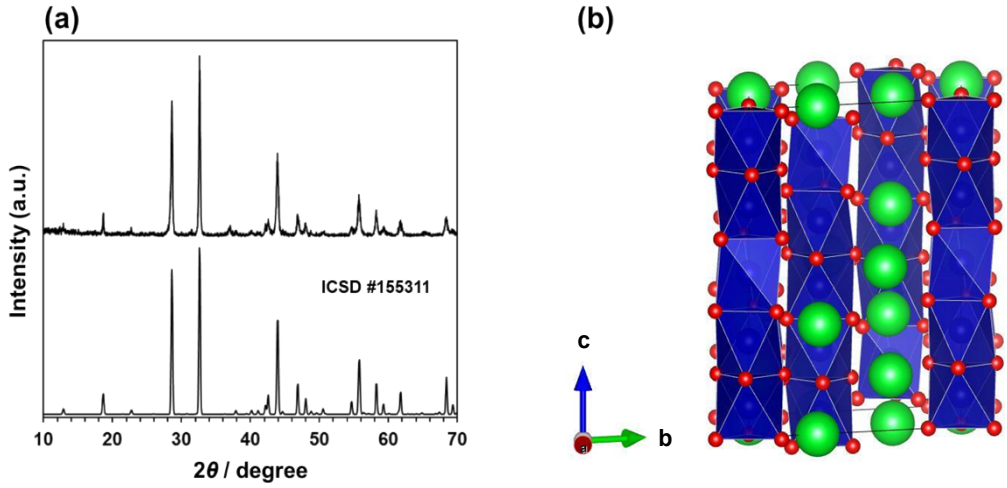

Figure S9. (a) XRD patterns and (b) crystal structure of $Sr_6Co_5O_{15}$.

Table S2. Results of Le Bail refinement of $SrTi_{1-x}Co_xO_3$.

x	*a* (Å)	R_{wp}
0	3.90557(2)	3.92
0.02	3.90370(1)	3.88
0.05	3.90152(2)	3.80
0.1	3.89885(4)	6.06
0.2	3.89260(6)	8.69
0.3	3.88781(7)	9.70
0.4	3.88366(2)	5.12
0.5	3.87981(2)	4.74
0.6	3.87531(3)	5.94
0.8	3.86769(1)	6.85

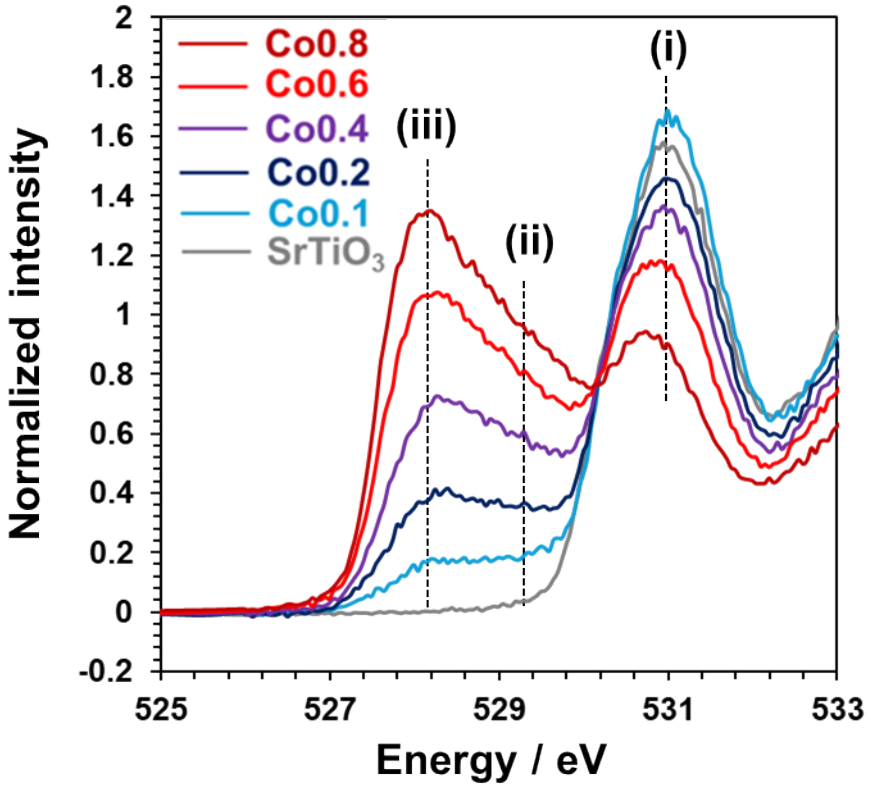

Figure S10. Magnified O *K*-edge XAS of $SrTi_{1-x}Co_xO_3$ (x = 0, 0.1, 0.2, 0.4, 0.6, 0.8) obtained in the PFY mode. Peaks (i) and (ii) show Ti 3*d* t_{2g}–O 2*p* hybridized states and Co 3d_{yz}/Co 3$d_{x^2-y^2}$–O 2*p* hybridized states, respectively.[29–31] Peak (iii) shows the O 2*p* ligand hole and Co 3d_{xy}/Co 3d_{xz}–O 2*p* hybridized states.[31]